Tuning the pinning energy in layered superconductors

R. J. Drost
Kamerlingh Onnes Laboratorium, Leiden University, P.O. Box 9506, 2300 RA Leiden, The Netherlands

C. J. van der Beek
Laboratoire des Solides Irradiés, Ecole Polytechnique, 91128 Palaiseau, France

H. W. Zandbergen
Laboratory of Materials Science, Delft University of Technology, Rotterdamseweg 137, 2628 AL Delft, The Netherlands

M. Konczykowski
Laboratoire des Solides Irradiés, Ecole Polytechnique, 91128 Palaiseau, France

A. A. Menovsky
Van der Waals-Zeeman Laboratory, University of Amsterdam, Valckeniersstraat 65, 1018 XE Amsterdam, The Netherlands

P. H. Kes
Kamerlingh Onnes Laboratorium, Leiden University, P.O. Box 9506, 2300 RA Leiden, The Netherlands
(Received 6 January 1999)

Reversible magnetization measurements show that the pinning energy of vortices localized on amorphous tracks created in $Bi_2Sr_2CaCu_2O_8$ single crystals by heavy-ion irradiation can be adjusted by altering the irradiation angle. The pinning energy is found to be proportional to the cross-sectional area of the defects in the CuO_2 planes. Both this size dependence and the observed quadratic temperature dependence of the pinning energy imply a predominant vortex core pinning interaction of pancake vortices with columnar defects as opposed to an electromagnetic pinning mechanism. An independent determination of the value of the Ginzburg-Landau coherence length is also presented. [S0163-1829(99)00321-5]

Fundamental studies of flux pinning and critical currents in (high temperature) superconductors (HTSC's) require pinning-center configurations with well-defined properties. Amorphous columnar defects (CD's) produced in HTSC's by heavy ion–irradiation[1–3] (HII) are among these because their size, physical properties, and spatial distribution can be well characterized by high-resolution electron microscopy (HREM) and scanning tunneling microscopy. The circular cross section of the ion tracks, of size comparable to that of the vortex core, facilitates an estimate of the elementary pinning energy and pinning force;[4–8] the irradiation dose determines the average concentration, usually expressed in terms of the dose equivalent field $B_\phi = \Phi_0 n_d$, where Φ_0 is the flux quantum and n_d is the areal density of CD's. Furthermore, in layered systems such as $Bi_2Sr_2CaCu_2O_8$, the background *pinscape* at high temperature is virtually smooth so that the pinning properties are especially well defined.

This paper will concentrate on an additional property of CD's, unique to layered superconductors, which can easily be realized experimentally. Since the order-parameter magnitude in the intermediate BiO layers is very small, vortices in $Bi_2Sr_2CaCu_2O_8$ should be viewed as stacks of ''pancake'' vortices in the superconducting CuO_2 double layers. Only those defects that reside in the CuO_2 layers can therefore be expected to be effective pinning centers. As for CD's, only their intersection with these layers will be relevant. This will be explicitly demonstrated below: we will show that the pancake pinning energy is proportional to the damaged area in the CuO_2 planes, when this is varied by irradiation in different directions.

The pinning energy per unit length U_0 of a vortex trapped on a CD of radius c_0 consists of a core contribution U_0^c and an electromagnetic part $U_0^{\rm em}$. The latter arises because of the modification of the vortex current when the vortex core is replaced by an amorphous track. It is important only when the track radius exceeds that of the vortex core, i.e., $c_0 \gg \sqrt{2}\xi_{ab}$, and is given by[4–7]

$$U_0^{\rm em} \approx \varepsilon_0 \ln\left(\frac{c_0}{\sqrt{2}\xi_{ab}}\right), \quad c_0 \gg \sqrt{2}\xi_{ab}. \tag{1}$$

Here $\varepsilon_0 = 2\pi\mu_0 H_c^2 \xi_{ab}^2 = \Phi_0^2/4\pi\mu_0\lambda_{ab}^2$, H_c is the thermodynamic critical field, λ_{ab} is the Ginzburg-Landau (GL) penetration depth, and ξ_{ab} is the GL coherence length. In the case where $c_0 \ll \sqrt{2}\xi_{ab}$ the core contribution dominates. It is proportional to the core fraction taken up by the columnar track, and can be estimated as[6,7]

$$U_0^c \approx \varepsilon_0 \left(\frac{c_0}{2\xi_{ab}}\right)^2, \quad c_0 \ll \sqrt{2}\xi_{ab}. \tag{2}$$

In Ref. 8 both core and electromagnetic contributions are computed by numerically solving the GL equations. The results for small c_0 agree well with Eq. (2).

From the direct determination of the pancake pinning energy as function of irradiation angle and temperature, it will

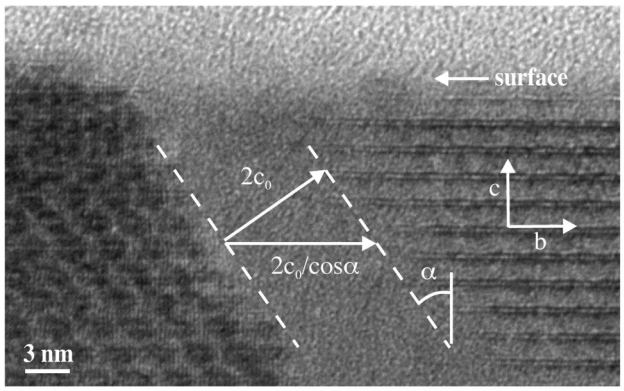

FIG. 1. HREM picture taken along the crystallographic a axis of a Bi-2212 sample irradiated with 6 GeV Pb ions at an angle $\alpha = 45°$ with respect to the c axis. The arrows indicate the track diameter $2c_0$ and its projection in the ab plane, $2c_0/\cos\alpha$.

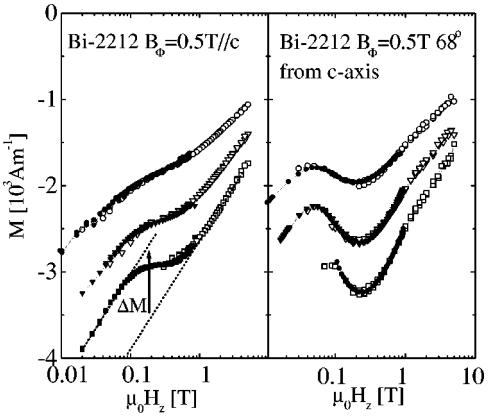

FIG. 2. Equilibrium magnetization curves for $Bi_2Sr_2CaCu_2O_8$ crystals irradiated at angles $\alpha = 0°$ (left-hand panel) and 68° (right-hand panel) with respect to the c axis ($B_\Phi = 0.5$ T). Temperatures are 72 K (□), 76 K (▽), and 80 K (○). Full symbols denote torque data whereas the open symbols are the results of SQUID measurements ($H \| c$ axis). The arrow and the dotted lines illustrate the construction used for the determination of the pinning energy.

turn out that Eq. (2) rather than Eq. (1) is obeyed in heavy-ion irradiated $Bi_2Sr_2CaCu_2O_8$, and hence, that $\xi_{ab} \gg c_0$. This has several implications: (i) core pinning is more important than electromagnetic pinning (ii) it provides an independent method to estimate the value of ξ_{ab}, still uncertain because thermal fluctuations prohibit the unambiguous determination of the upper critical field $B_{c2} = \Phi_0/2\pi\xi_{ab}^2$. (iii) it is, in principle, possible to tailor yet more efficient pinning centers by introducing cylindrical voids of larger diameter.

The experiments have been performed on several $Bi_2Sr_2CaCu_2O_8$ single crystals from the same batch, grown by the traveling-solvent floating-zone technique[9] (typical dimensions: $\sim 2\times 2\times 0.04$ mm^3). The crystals were post-annealed (800 °C in air) and quench cooled to ensure a homogeneous oxygen content. All samples had $T_c = 90$ K; the London penetration depth determined from the logarithmic slope of the magnetization $\partial M/\partial \ln H$ at high fields[10] is $\lambda_L(0) = \lambda_{ab}(0)\sqrt{2} = 245$ nm (H is the applied field). A magneto-optical characterization of the flux penetration confirmed the homogeneity of the samples and the absence of extended defects. The crystals were irradiated simultaneously at GANIL (Caen, France) with a beam of 6 GeV Pb ions, to a dose $n_d = 2.5\times 10^{10}$ cm^{-2}, or $B_\phi = 0.5$ T. For each crystal, the ion beam was oriented along a different direction: the nominal angles between the beam and the c axis were $\alpha = 0°$, 30°, 45°, and 60°, respectively. The kinetic energy of the Pb ions (6 GeV) ensures that for all angles α the entire specimen is traversed. The actual angles α were determined *a postiori* by means of Hall probe magnetometry.[11] The actual irradiation angle is the angle where the ac shielding current was maximum in an ac transmittivity measurement as function of applied field angle;[11] they were found to be 0°, 26°, 45°, and 68°, respectively. These results combined with measurements of the irreversibility line of the various samples used in this paper will be presented in a separate paper.[12]

The defect structure created by the swift heavy ions was visualized by HREM.[13] A typical result, obtained on the sample irradiated at $\alpha = 45°$, is shown in Fig. 1, which reveals the damaged area created by a heavy-ion impact in the crystallographic (b,c) plane. The ion creates an amorphous track with radius $c_0 \sim 3.5$ nm, oriented at $\sim 45°$ with respect to the ab planes. This implies that the intersection of the track with the CuO_2 planes is elongated in the b direction; it is larger than the track radius by a factor $1/\cos\alpha$. As a consequence, the cross-sectional area of the track in the CuO_2 planes is ellipsoidal with area $\pi c_0^2/\cos\alpha$.

Vortex pinning energies were determined by measuring the equilibrium magnetization $M_{\rm eq}$ (Refs. 14,15) with the use of (i) a rotation experiment in a (noncompensated) homebuilt capacitive torquemeter and (ii) a commercial superconducting quantum interference device (SQUID) magnetometer (Quantum Design MPMS-5S) with the field parallel to the c axis. For experimental details, we refer to Ref. 15. Figure 2 shows the equilibrium magnetization curves of the samples irradiated at 0° and 68° for various temperatures. This figure shows both the SQUID and torque data. For the latter measurements we have used the same analysis as presented in Refs. 15,16: in a layered superconductor $M_{\rm eq}$ only has a component $M_{\rm eq}^z$ along the c axis, which can be obtained from the torque per unit volume τ as $M_{\rm eq}^z = \tau/H_x = \tau/H\cos\Theta$; here Θ is the angle between the field and the ab plane. The near-perfect collapse of $M_{\rm eq}^z$ obtained from torque (with H oriented away from the c axis) and with the SQUID (where $H \| c$) in Fig. 2 shows that the magnetic moment is indeed oriented uniquely along the c direction.[15] Moreover, the magnetization depends only on the field component parallel to the c axis H_z, i.e., it is solely determined by the density of pancake vortices in the CuO_2 planes.

The reversible magnetization of all samples exhibits the typical behavior found after heavy-ion irradiation: a minimum and a maximum develop in $|M_{\rm eq}|$ as the temperature is decreased. However, the effects of the irradiation are more pronounced for higher irradiation angles (Figures 2 and 3 where the isothermal magnetization at 76 K is plotted for all samples). The shift of the inflection point in $|M_{\rm eq}|$ to lower H as α is increased, is correlated with the effective matching field $B_\phi^{\rm eff} = B_\phi\cos\alpha$, determined by the density of CD intersections with the CuO_2 planes (for example, for $\alpha = 68°$, $B_\phi^{\rm eff} = 0.19$ T). This illustrates the pancake stacklike nature of vortices in $Bi_2Sr_2CaCu_2O_8$ since only the areal density of

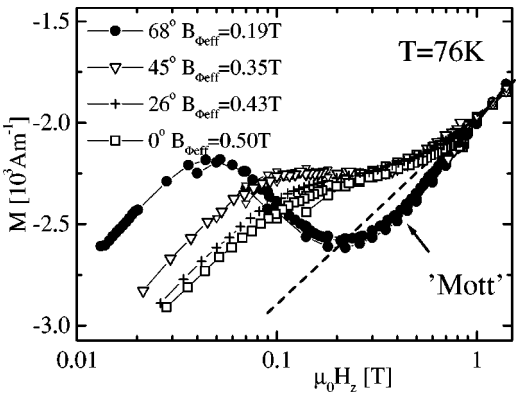

FIG. 3. Isothermal equilibrium magnetization curves ($T=76$ K) for crystals irradiated at four different angles indicated in the plot. Both SQUID and torque data are shown.

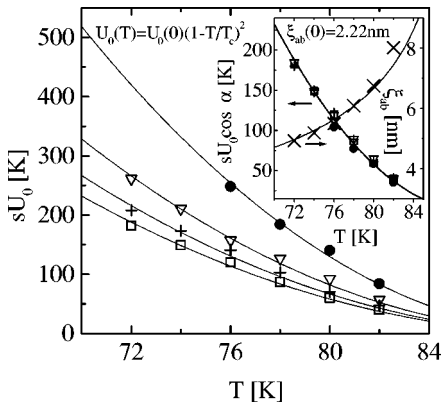

FIG. 4. The pinning energy per pancake vortex for crystals irradiated at 0° (□), 26° (+), 45° (▽), and 68° (●), obtained from the procedure illustrated in the left-hand panel of Fig. 2. Lines are fits to the function $U_0(0)s(1-T/T_c)^2$ with $T_c=90$ K. Inset: the same data multiplied by a factor $\cos\alpha$. Also plotted is the result for $\xi_{ab}(T)$ (×) determined from the $\alpha=0°$ data. The solid line represents the fit to $\xi_{ab}(T)=\xi_{ab}(0)/(1-T/T_c)^{1/2}$.

columnar defects in the CuO_2 planes is important. In all cases, $M_{\rm eq}$ follows the usual London behavior at fields well in excess of B_ϕ, i.e., the magnetization versus the logarithm of field is linear:

$$M_{\rm eq}\propto\frac{\varepsilon_0}{2\Phi_0}\ln\left(\frac{\eta B_{c2}}{B}\right). \tag{3}$$

A theoretical value for the parameter $\eta\approx0.35$ can only be obtained as a numerical estimate.[17] The high-field behavior corresponds to the entry of ''free'' vortices, i.e., those that are not trapped by a columnar defect.[14] Note the collapse of the data for the different samples at high fields. At high irradiation doses — much higher than used here — $|M_{\rm eq}|$ at fields $\mu_0H\gg B_\phi$ may in fact be decreased by the irradiation due to the missing superconducting fraction induced by the insulating columns. However, such effects are not prominent at $B_\phi<1$ T.[14]

At fields $\mu_0H\ll B_\phi$, a London-like behavior is also observed, with a slope nearly similar to the slope at high fields. In this regime, $M_{\rm eq}$ is determined by the addition of vortices that do become trapped on a column.[14,15,18] The pinning energy per unit length U_0 can be simply obtained from the difference between the downward extrapolation of the high-field limit of the magnetization curve and the low-field magnetization, as shown in Fig. 2. The resulting values, expressed as the pinning energy per vortex per CuO_2 double layer, $U_0s=\Phi_0s\Delta M$ (s is the distance between double layers), are shown in Fig. 4 for the different samples. The enhancement of the pinning energy as the column direction is rotated away from the c axis is clear. In fact, the pinning energy for $\alpha=68°$ is more than double that for $\alpha=0$. The inset to Fig. 4 shows that when multiplied by a factor $\cos\alpha$, the $U_0(T)s$ curves for all crystals overlap. This means that U_0 is proportional to the cross-sectional area of the columnar defects with the CuO_2 double layers, i.e., $U_0\propto\pi c_0^2/\cos\alpha$. By implication, only the damaged area in the CuO_2 layers contributes to pinning. Moreover, the proportionality of U_0 to this area means that the core term U_0^c is dominant. In that case, the factor c_0^2 in Eq. (2) should be replaced by $c_0^2/\cos\alpha$ yielding the experimentally measured dependence of the pinning energy:

$$U_0s\approx\varepsilon_0s\left(\frac{c_0}{\xi_{ab}}\right)^2\frac{1}{2\cos\alpha}. \tag{4}$$

The temperature dependence of U_0^c is given by the product of $\xi_{ab}^{-2}\propto(1-t)$ and $\varepsilon_0\propto\lambda_{ab}^{-2}\propto(1-t)$, resulting in $U_0^c(T)s=U_0^c(0)s(1-t)^2$ (with $t\equiv T/T_c$). We note that the temperature dependence of a purely electromagnetic pinning energy would be linear: $U_0^{\rm em}(T)s=U_0^{\rm em}(0)s(1-t)$. It is seen in Fig. 4 that the quadratic temperature dependence with $T_c=90$ K fits the data quite well. It yields $U_0(0)s=4.7\times10^3$ K and 10.5×10^3 K for the samples irradiated at 0° and 68°, respectively. The quadratic temperature dependence of the pinning energy and its scaling with the defected intersection area of columns with the CuO_2 layers leads to the conclusion that at elevated temperatures *core pinning is dominant over the electromagnetic pinning mechanism*.

The proportionality of the pinning energy to the ratio $(c_0/\xi)^2$ provides a method to determine $\xi_{ab}(T)$ independent of the value of λ_{ab}. This can be achieved by dividing the high-field logarithmic slope of the magnetization $\partial M/\partial\ln H=\varepsilon_0/2\Phi_0$ [Eq. (3)] by ΔM

$$\frac{1}{\Delta M}\frac{\partial M}{\partial\ln H}=\frac{\Phi_0}{\varepsilon_0}\left(\frac{2\xi}{c_0}\right)^2\frac{\varepsilon_0}{2\Phi_0}=2\left(\frac{\xi}{c_0}\right)^2. \tag{5}$$

Taking the square root and using the value $c_0=3.5$ nm taken from HREM images yields the $\xi(T)$ curve depicted in the inset to Fig. 4. A fit to the GL temperature dependence $\xi(T)=\xi(0)(1-t)^{-1/2}$ gives $\xi_{ab}(0)=2.2$ nm, and from that $B_{c2}(0)=66$ T, and $(\partial B_{c2}/\partial T)_{T=T_c}\approx-1.05$ T/K. This procedure for the determination of ξ_{ab} has several important advantages: first of all, no extrapolation approach (with only logarithmic accuracy) is needed.[20] In addition, it is independent of the value of the parameter η appearing in Eq. (3). The value $\xi_{ab}=2.2$ nm implies that core pinning is predominant at temperatures $T\gtrsim35$ K. This excludes the interpretation of features in the irreversibility line as being the consequence of a crossover between electromagnetic pinning and core pinning.[21]

Armed with the above information, we return to the shape of the equilibrium magnetization curves for different irradiation angles, see Fig. 3. Note that the samples irradiated at a high angle (e.g., $\alpha = 68°$) display a much sharper increase of $|M_{eq}|$ near B_ϕ^{eff} than the sample irradiated along c. This means that the compression modulus ($c_{11} \propto \delta H/\delta B$) increases dramatically with larger pinning energy. It is also seen that for $\alpha = 68°$, the magnetization $|M_{eq}|$ near B_ϕ actually *exceeds* the value of $|M_{eq}|$ before irradiation. Both features can be interpreted as being a remnant of the Mott insulator phase postulated in Ref. 6. In this phase all vortices are locked onto a column and the compressibility ($\propto c_{11}^{-1}$) of the vortex system is zero leading to a fixed induction over a finite field interval. Although the interplay between the random positions of the CD's and intervortex interactions prevents the occurrence of a true Mott insulator,[19] the relative increase in pinning energy with respect to the intervortex interaction for higher α drives the system closer to the Mott insulator phase. We note that the features of the Mott insulator phase should be more pronounced at very low temperatures where the pinning energy of CD's exceeds all other energy scales. In this temperature regime, however, the equilibrium magnetization curve cannot be measured since it is completely masked by strong irreversibility.

In conclusion, the pinning energy in layered superconductors with amorphous columnar defects can be tuned by heavy-ion irradiation under different angles. The pinning energy is proportional to the area of the intersection of a track with the CuO_2 planes and follows a $(1-t)^2$ temperature dependence, which shows that only core pinning of pancake vortices is effective. Changing the track cross section provides a means to determine ξ_{ab}, a value $\xi_{ab}(0) = 2.2$ nm is found. The small size of the column radius with respect to the coherence length means that it should, in principle, be possible to attain yet higher pinning energies by introducing cylindrical voids of slightly larger cross section than can be obtained by heavy-ion irradiation.

This work was supported in part by the Nederlandse Stichting F.O.M., which is financially supported by NWO.

[1] L. Civale *et al.*, Phys. Rev. Lett. **67**, 648 (1991).
[2] M. Konczykowski *et al.*, Phys. Rev. B **44**, 7167 (1991).
[3] W. Gerhäuser *et al.*, Phys. Rev. Lett. **68**, 879 (1992).
[4] G.S. Mkrtchyan and V.V. Shmidt, Zh. Éksp. Teor. Fiz. **61**, 367 (1971) [Sov. Phys. JETP **34**, 195 (1972)].
[5] A.I. Buzdin and D. Feinberg, Physica C **235-240**, 2755 (1994).
[6] D.R. Nelson and V.M. Vinokur, Phys. Rev. B **48**, 13 060 (1993).
[7] G. Blatter *et al.*, Rev. Mod. Phys. **66**, 1125 (1994).
[8] N. Takezawa and K. Fukushima, Physica C **228**, 149 (1994).
[9] T.W. Li *et al.*, J. Cryst. Growth **135**, 481 (1994).
[10] T.W. Li *et al.*, Physica C **257**, 179 (1996).
[11] C.J. van der Beek *et al.*, Phys. Rev. Lett. **74**, 1214 (1995).
[12] C.J. van der Beek *et al.* (unpublished).
[13] C. Træholt *et al.*, Physica C **290**, 239 (1997).
[14] C.J. van der Beek *et al.*, Phys. Rev. B **54**, R792 (1996).
[15] R.J. Drost *et al.*, Phys. Rev. B **58**, R615 (1998).
[16] J.C. Martinez *et al.*, Phys. Rev. Lett. **69**, 2276 (1992).
[17] A.E. Koshelev, Phys. Rev. B **50**, 506 (1994).
[18] L.N. Bulaevskii, V.M. Vinokur, and M.P. Maley, Phys. Rev. Lett. **77**, 936 (1996).
[19] C. Wengel and U.C. Täuber, Phys. Rev. Lett. **78**, 4845 (1997); Phys. Rev. B **58**, 6565 (1998).
[20] V.G. Kogan *et al.*, Phys. Rev. Lett. **70**, 1870 (1993).
[21] D. Zech *et al.*, Phys. Rev. B **54**, 6129 (1996).